Constraining parameters of magnetic field decay for accreting isolated neutron stars

S. B. Popov
Sternberg Astronomical Institute
Universitetskii pr.13, 119899, Moscow, Russia
e-mail: polar@sai.msu.ru
and
M. E. Prokhorov
Sternberg Astronomical Institute
Universitetskii pr.13, 119899, Moscow, Russia
e-mail: mystery@sai.msu.ru

Abstract

The influence of exponential magnetic field decay (MFD) on the spin evolution of isolated neutron stars is studied. The ROSAT observations of several X-ray sources, which can be accreting old isolated neutron stars, are used to constrain the exponential and power-law decay parameters. We show that for the exponential decay the ranges of minimum value of magnetic moment, μ_b, and the characteristic decay time, t_d, $\sim 10^{29.5} \geq \mu_b \geq 10^{28}\,\mathrm{G\,cm^3}$, $\sim 10^8 \geq t_d \geq 10^7$ yrs are excluded assuming the standard initial magnetic moment, $\mu_0 = 10^{30}\,\mathrm{G\,cm^3}$. For these parameters, neutron stars would never reach the stage of accretion from the interstellar medium even for a low space velocity of the stars and a high density of the ambient plasma. The range of excluded parameters increases for lower values of μ_0.

We also show, that, contrary to exponential MFD, no significant restrictions can be made for the parameters of power-law decay from the statistics of isolated neutron star candidates in ROSAT observations.

Isolated neutron stars with constant magnetic fields and initial values of them less than $\mu_0 \sim 10^{29}\,\mathrm{G\,cm^3}$ never come to the stage of accretion.

We briefly discuss the fate of old magnetars with and without MFD, and describe parameters of old accreting magnetars.

Keywords: stars: neutron stars – magnetic fields: decay – accretion

1 Introduction

Astrophysical manifestations of neutron stars (NSs) are determined by their periods and magnetic fields. Four main evolutionary stages of isolated NSs can be singled out (see e.g. (Lipunov, 1992) for more details): the *ejector*, the *propeller*, the *accretor* and the *georotator*.

On average NSs should have high spatial velocities due to an additional kick obtained during the supernova explosion (Lyne and Lorimer, 1994, Lorimer et al., 1997). The interstellar medium (ISM) accretion rate for high velocity objects should be rather low. However, recent population synthesis calculations (Popov et al., 2000) indicate that several old accreting NSs can be observed in the solar vicinity even for the space velocity distribution similar to one derived from radio pulsar observations.

Magnetic field decay (MFD) in NSs is a matter of controversy. Many models of the MFD have been proposed starting from the first simple models (Gunn and Ostriker, 1970) up to the recent calculations (Sang and Chanmugam, 1990; Urpin and Muslimov, 1992). Observations of radio pulsars (Lyne et al., 1998) give no evidence for MFD with characteristic time scales t_d shorter than $\sim 10^7$ yrs. Here we suggest to use old accreting isolated neutron stars as probes of the models of field decay and try to put some limits on the parameters of the exponential and power-law MFD on a longer time scale assuming that some X-ray sources observed by ROSAT are indeed old accreting isolated NSs (Haberl et al., 1998; Neühauser and Trümper, 1999; Schwope et al., 1999).

This presentation is based mainly on two our recent papers (Popov and Prokhorov, 2000a,b).

2 Calculations and results

The main idea is to calculate the ejector time, i.e. a time interval spent by a NS on the ejector stage, for different parameters of the MFD and, using standard assumptions for the initial NS parameters, to compare this time with the Hubble time, t_H.

The ejector time, t_E, monotonically increases with increasing velocity of NS, v, and decreasing density of the ISM, n. For a constant magnetic field of a NS this relation takes the simple form:

$$t_E(\mu = const) \sim 10^9 \mu_{30}^{-1} n^{-1/2} v_{10}\,\mathrm{yrs}. \tag{1}$$

Using a high mean ISM density $n \sim 1\mathrm{cm}^{-3}$ and a low space velocity of NSs (about the sound speed in the ISM), $v \sim 10\,\mathrm{kms}^{-1}$, we arrive at the lower limit of t_E. After the ejection stage has been over, the NS passes to the propeller stage and only after that can become an accreting X-ray source. The duration of the propeller stage t_P is poorly known, but for a constant magnetic field t_P is always less than t_E, (see Lipunov and Popov, 1995). Therefore if for some parameters of a NS t_E exceeds the Hubble time $t_H \simeq 10^{10}$ yrs, it can not come to the accretion stage and hence can not underly the ROSAT INS candidate.

We note, that if the initial magnetic moment of a NS is about $\mu_0 \sim 10^{29}$ G cm^3 or smaller, than (in the case of constant field) this star never leave the ejector stage even for low velocity and high ISM density! So, significant part of INS for any velocity distribution can't become accretors at all.

In addition, we assumed that NSs are born with sufficiently small rotational periods, p_0, and all have the same parameters of the MFD. We shall consider different initial surface magnetic field values.

2.1 Exponential decay

The field decay in this subsection is assumed to have an exponential shape:

$$\mu = \mu_0 \cdot e^{-t/t_d},\ \mathrm{for}\ \mu > \mu_b \tag{2}$$

where μ_0 is the initial magnetic moment ($\mu = \frac{1}{2} B_p R_{NS}^3$, here B_p is the polar magnetic field, R_{NS} is the NS radius), t_d is the characteristic time scale of the decay, and μ_b is the bottom value of the magnetic moment which is reached at the time t_{cr}:

$$t_{cr} = t_d \cdot \ln\left(\frac{\mu_0}{\mu_b}\right), \tag{3}$$

and does not change after that.

In Fig. 1 we show as an illustration the evolutionary tracks of NSs on $P - B$ diagram for $v = 10\,\mathrm{km\,s}^{-1}$ and $n = 1\,\mathrm{cm}^{-3}$. Tracks start at $t = 0$ when $p = 20$ms and $\mu = 10^{30}\mathrm{G\,cm}^3$ and end at $t = t_H = 10^{10}$ yrs (for $t_d = 10^7$ yrs and $t_d = 10^8$ yrs) or at the moment when $p = p_E$ (for

$t_d = 10^9$yrs, $t_d = 10^{10}$ yrs and for a constant magnetic field) . The line with diamonds shows $p = p_E(B)$.

The ejector stage ends when the critical ejector period, p_E, is reached:

$$p_E = 11.5\, \mu_{30}^{1/2} n^{-1/4} v_{10}^{1/2}\ \mathrm{s}, \tag{4}$$

where $v_{10} = \sqrt{v_p^2 + v_s^2}/10\,\mathrm{km\,s^{-1}}$. v_p is the NS's spatial velocity, v_s and n are the sound velocity and density of the ISM, respectively. In the estimates below we shall assume $v = 10\ \mathrm{km\,s^{-1}}$ and $n = 1\ \mathrm{cm^{-3}}$.

The initial NSs' spin periods should be taken much smaller than p_E. Here to calculate duration of the ejection stage we assume $p_0 = 0$ s. To compute this time we used the magnetodipole formula:

$$\frac{dp}{dt} = \frac{2}{3}\frac{4\pi^2\mu^2}{pIc^3}, \tag{5}$$

where μ can be a function of time.

After a simple algebra we arrive at the following expression for t_E:

$$t_E = \begin{cases} -t_d \cdot \ln\left[\dfrac{T}{t_d}\left(\sqrt{1+\dfrac{t_d^2}{T^2}} - 1\right)\right],\ t_E < t_{cr} \\ t_{cr} + T\dfrac{\mu_0}{\mu_b} - t_d\dfrac{1}{2}\left(\dfrac{\mu_0}{\mu_b}\right)^2\left(1 - e^{-2t_{cr}/t_d}\right), \\ \qquad\qquad t_E > t_{cr} \end{cases} \tag{6}$$

where the coefficient T (which is just t_E for constant magnetic field) is determined by the formula:

$$T = \frac{3Ic}{2\mu_0\sqrt{2v\dot{M}}} \simeq 10^{17} I_{45}\mu_{0_{30}}^{-1} v_{10}^{-1/2}\dot{M}_{11}^{-1/2}\ \mathrm{s}. \tag{7}$$

Here $\dot{M}$ can be formally determined according to the Bondi equation for the mass accretion rate even if the NS is not at the accretion stage:

$$\dot{M} \simeq 10^{11}\, n v_{10}^{-3}\,\mathrm{g\,s^{-1}}. \tag{8}$$

The results of calculations of t_E for several values of μ_0 and t_d are shown in Fig. 2. The right end points of all curves are limited by the values $\mu_b = \mu_0$. These points correspond to the evolution of a NS with constant magnetic field (see eq. (2)) and for them $t_E = T$. One can see the increase of t_E for evolution with a constant field for smaller initial fields.

If μ_b is small enough, the NS field has no time to reach the bottom value. In this case t_E is determined by the 1st branch of equation (6) and does not depend on μ_b. In Fig. 2 this situation corresponds to the left horizontal parts of the curves. At

$$\mu_b > \mu_0 \left[\frac{T}{t_d} \left(\sqrt{1 - \frac{t_d^2}{T^2}} - 1 \right) \right]$$

the situation changes so that t_E starts to depend on μ_b. In this region two counter-acting factors operates. On the one hand, the NS braking becomes slower with decreasing μ (see eq. (5)). On the other hand, the end period of the ejection p_E becomes shorter (4). Since $t_E < T$ at the left hand side horizontal part and $(dT_E/d\mu_b)|_{\mu_0} < 0$, the right hand side of the curve must have a maximum. The first factor plays the main role to the right of the maximum. The magnetic field there rapidly falls down to μ_b at $p \ll P_E$ and most time NS evolves with the minimum field $\mu = \mu_b$ (this time period increases with decreasing μ_b). To the left of the maxium but before the horizontal part the NS's magnetic field reaches $\mu = \mu_b$ with the spin period close to p_E (the smaller μ_b, the closer) and soon after $t = t_{cr}$ the NS leaves the ejection stage.

As it is seen from this Figure, for some combination of parameters t_E is longer than the Hubble time. It means that such NSs never evolve further than the ejection stage.

We argue that since accreting isolated NSs are really observed, the combinations of t_d and μ_b for which no accreting isolated NS appear can be excluded for the progenitors of ROSAT X–ray sources. The regions of excluded parameters are plotted in Figs. 3 and 4.

The hatched regions correspond to parameters for which t_E is longer than 10^{10} yrs, so a NS with such parameters never comes to the accretor stage and hence can not appear as an accreting X-ray source. In view of the fact of observations of accreting old isolated NSs by ROSAT satellite, this region can be called "forbidden" for a given μ_0.

In the "forbidden" region in Fig. 3, which is plotted for $\mu_0 = 10^{30}\,\mathrm{G\,cm}^3$, all NSs reach the bottom field in a Hubble time or faster, and the evolution on late stages proceeds with the minimal field. The left hand side of the forbidden region is determined approximately by the condition

$$p_E(\mu_b) = p(t = t_{cr}). \qquad (9)$$

The right hand side of the region is roughly determined by the value of μ_b, with which a NS can reach the ejection stage for any t_d, i.e. this μ_b corresponds to the minimum value of μ_0 with which a NS reaches the ejection stage without MFD.

In Fig. 3 we also show the "forbidden" region for $\mu_0 = 0.5 \cdot 10^{30}\,\mathrm{G\,cm^3}$ (dotted line). The dashed line in Fig. 3 shows that for all interesting parameters a NS with $\mu_0 = 10^{30}\,\mathrm{G\,cm^3}$ reaches μ_b in less than 10^{10} yrs. The dash-dotted line shows the same for $\mu_0 = 0.5 \cdot 10^{30}\,\mathrm{G\,cm^3}$. The solid line corresponds to $p_E(\mu_b) = p(t = t_{cr})$, where $t_{cr} = t_d \cdot \ln(\mu_0/\mu_b)$. The physical sense of this line can be described in the following way. This line divides two regions: in the upper left region t_d are relatively long and μ_b relatively low, so NS can't reach bottom field during ejector stage; in the lower right region t_d are short and μ_b relatively high, so NS reach μ_b at the stage of ejection.

Fig. 4 is plotted for $\mu_0 = 10^{29}\,\mathrm{G\,cm^3}$. For long t_d ($> 4 \cdot 10^9$ yrs) the NS cannot leave the ejection stage for any $\mu_b \leq \mu_0$. That's why in the upper part of the figure a horizontal "forbidden" region appears.

2.2 Power-law decay

Power-law (as also exponential) MFD is a widely discussed variant of NSs' field evolution. Power-law is a good fit for several different calculations of the field evolution (Goldreich & Reisenegger, 1992; Geppert et al., 2000). The power-law MFD can be described with the following simple formula:

$$\frac{dB}{dt} = -aB^{1+\alpha}. \tag{10}$$

So, we have two parameters of decay: a and α. As far as this decay is relatively slow for the most interesting values of α greater/about 1 (we use the same units as in (Colpi et al., 2000)), we don't specify any bottom magnetic field, contrary to what we made for more rapid exponential decay (Popov & Prokhorov, 2000a). Even for the Model C from (Colpi et al., 2000) (see Table 1) with relatively fast MFD the magnetic field can decrease only down to $\sim 10^8$ G in 10^{10} yrs (see Fig. 5). But for very small α the magnetic field can decay significantly during the Hubble time for any reasonable value of a. And, probably, it is useful to introduce in the later case a bottom field.

At the stage of ejection an INS is spinning down according to the magnetodipole formula: $P\dot{P} \approx bB^2$. Here $b=3$, values of magnetic field, B, B_∞ and B_0, are taken in units 10^{13} G and time, t, in units 10^6 yrs (as in Colpi et al., 2000).

In the table we show parameters of the Models A, B, C from (Colpi et al., 2000). B_∞ is the magnetic field calculated for $t=t_{Hubble}=10^{10}$ yrs and for the initial field $B_0=10^{12}$ G. Models A and B correspond to ambipolar diffusion in the irrotational and the solenoidal modes respectively. Model C describes MFD in the case of the Hall cascade (models are valid mostly for relatively high values of magnetic field).

Table 1: Models A,B,C from (Colpi et al., 2000)

Model	A	B	C
a	0.01	0.15	10
α	5/4	5/4	1
B_∞	$\approx 1.9\cdot 10^{11}$ G	$\approx 2.4\cdot 10^{10}$ G	$\approx 10^8$ G

In Fig. 6 we show dependence of the ejector period, p_E, and the asymptotic period, p_∞, on the parameter a for $\alpha=1$ for different values of the initial magnetic field, B_0:

$$p_E = 25.7\, B_\infty^{1/2} n^{-1/4} v_{10}^{1/2}\ \mathrm{s}, \tag{11}$$

$$p_\infty^2 = \frac{2}{2-\alpha}\frac{b}{a} B_0^{2-\alpha}. \tag{12}$$

Here p_E was calculated for $t=t_{Hubble}=10^{10}$ yrs, i.e. for the moment, when $B=B_\infty$.

It is clear from Fig. 6, that for the initial field greater/about 10^{11} G low velocity INSs are able to come to the stage of accretion: for $B_0=10^{11}$ G lines for p_∞ and p_E for the lowest possible velocity, 10 km/s, coincides.

For power-law decay we can also plot "forbidden" regions on the plane a–α, where an INS for a given velocity for sure cannot come to the stage of accretion in the Hubble time (see Popov & Prokhorov, 2000b). If one also takes into account the stage of propeller (between ejector and accretor stages) it becomes clear, that "forbidden" regions for an INS which cannot reach the stage of accretion are even larger.

For the most interesting cases (Models A, B, C from (Colpi et al., 2000)) and $v < 200$ km/s INSs can reach the stage of accretion. It is an important point, that fraction of low velocity NSs is very small (Popov et al., 2000) and most of NSs have velocities about 200 km/s.

3 Evolved magnetars

In the last several years a new class of objects - highly magnetized NSs, *"magnetars"* (Duncan and Thompson, 1992) – became very popular in connection with soft γ-repeaters (SGR) and anomalous X-ray pulsars (AXP) (see Mereghetti and Stella, 1995; Kouveliotou et al., 1999; Mereghetti, 1999 and recent theoretical works Alpar, 1999; Marsden et al., 2000; Perna et al., 2000).

Magnetars come to the propeller stage with periods $\sim 10 - 100$ s in the Models A, B, C (see Fig. 2 in Colpi et al., 2000). Then their periods quickly increase, and NSs come to the stage of accretion with significantly longer periods, and at that stage they evolve to a so-called equilibrium period (Lipunov and Popov, 1995; Konenkov and Popov, 1997) due to accretion of the turbulent ISM:

$$p_{eq} \sim 2800 B_{13}^{2/3} I_{45}^{1/3} n^{-2/3} v_{10}^{13/3} v_{t_{10}}^{-2/3} M_{1.4}^{-8/3} \text{ s} \tag{13}$$

Here v_t is a characteristic turbulent velocity, I – moment of inertia, M – INS's mass. This formula underestimate the period for relatively high v_t, and relatively low v, because it assumes, that all external angular moment can be accreted by a INS.

Isolated accretor can be observed both with positive and negative sign of $\dot{p}$ (Lipunov and Popov, 1995). Spin periods of INSs can differ significantly from p_{eq} contrary to NSs in disc-fed binaries, and similar to NSs in wide binaries, where accreted matter is captured from giant's stellar wind. It happens because spin-up/spin-down moments are relatively small.

As the field is decaying the equilibrium period is decreasing, coming to ~ 28 sec when the field is equal to 10^{10} G (we note here recently discovered objects RX J0420.0-5022 (Haberl et al., 2000) with spin period ~ 22.7 s).

It is important to discuss the possibility, that evolved magnetar can appear also as a georotator. It happens if:

$$v > 300 B_{13}^{-1/5} n^{1/10}\,\mathrm{km/s}. \tag{14}$$

For all values of a and α that we used NSs at the end of their evolution ($t = 10^{10}$ yrs) have magnetic fields $< 10^{12}$ G for wide range of initial fields, so they never appear as georotators if $v < 480$ km/s for $n = 1\mathrm{cm}^{-3}$. But without MFD magnetars with $B > 10^{15}$ G and velocities $v > 100$ km/s can appear as georotators.

Popov et al. (2000) showed, that georotator is a rare stage for INSs, because an INS can come to the georotator stage only from the propeller or accretor stage, but all these phases require relatively low velocities, and high velocity INSs spend most of their lives as ejectors. This situation is opposite to binary systems, where a lot of georotators are expected for fast stellar winds (wind velocity can be much faster than INS's velocity relative to ISM).

Without MFD magnetars also can appear as accreting sources. In that case they can have very long periods and very narrow accretion columns (that means high temperature). Such sources are not observed now. Absence of some specific sources associated with evolved magnetars (binary or isolated) can put some limits on their number and properties (dr. V. Gvaramadze drew our attention to this point).

At the accretion part of INSs' evolution periods stay relatively close to p_{eq} (but can fluctuate around this value), and INSs' magnetic fields decay down to $\sim 10^{10} - 10^{11}$ G in several billion years for the Models A and B. It corresponds to the polar cap radius about 0.15 km and temperature about 250 – 260 eV (the same temperature, of course, can appear for INSs evolving with constant field), higher than for the observed INS candidates with temperature about 50 – 80 eV. We calculate the polar cap radius, $R_{cap} = R_{NS}\sqrt{(R_{NS}/R_A)}$ (R_A - Alfven radius), with the following formula:

$$R_{cap} = 6 \cdot 10^3\, B_{13}^{-2/7} n^{1/7} v_{10}^{-3/7} R_{NS_6}^{3/2}\ \mathrm{cm}. \tag{15}$$

The temperature can be even larger, than it follows from the formula above as far as for very high field matter can be channeled in a narrow ring, so the area of the emitting region will be just a fraction of the total polar cap area.

As the field is decreasing the radius of the polar cap is increasing, and the temperature is falling. Sources with such properties (temperature about

250-260 eV) are not observed yet (Schwope et al., 1999). But if the number of magnetars is significant (about 10% of all NSs) accreting evolved magnetars can be found in the near future, as far as now we know about 5 accreting INS candidates (Treves et al., 2000; Neühauser and Trumper, 1999), and their number can be increased in future. $\dot{p}$ measurements are necessary to understand the nature of such sources, if they are observed.

Recently discovered object RX J0420.0-5022 (Haberl et al., 2000) with the spin period $\sim$ 22.7 s, can be an example of an INS with decayed magnetic field accreting from the ISM, as previously RX J0720.4-3125. Due to relatively low temperature, 57 eV, its progenitor cannot be a magnetar for power-law MFD (Models A,B,C) or similar sets of parameters, because a very large polar cap is needed, which is difficult to obtain in these models. Of course RX J0420.0-5022 can be explained also as a cooling NS. The question "are the observed candidates cooling or accreting objects?" is still open (see Treves et al., 2000). If one finds an object with $p > 100$ s and temperature about $50 - 70$ eV it can be a strong argument for its accretion nature, as far as such long periods for magnetars can be reached only for very high initial magnetic fields for reasonable models of MFD and other parameters.

4 Discussion and conclusions

We tried to evaluate the region of parameters which are excluded for models of the exponential and power-law MFD in NSs using the fact of observations of old accreting isolated NSs in X-rays.

For the exponential decay the intermediate values of t_d ($\sim 10^7 - 10^8$ yrs) in combination with the intermediate values of μ_b ($\sim 10^{28} - 10^{29.5}\,\mathrm{G\,cm^3}$) for $\mu_0 = 10^{30}\,\mathrm{G\,cm^3}$ can be excluded for progenitors of isolated accreting NSs because NSs with such parameters would always remain on the ejector stage and never pass to the accretion stage.

For high μ_0 NSs should reach t_E even for $t_d < 10^8$ yrs. For weaker fields the "forbidden" region becomes wider. The results are dependent on the initial magnetic field μ_0, the ISM density n, and NS velocity v.

In fact the limits obtained are very strong, because we did not take into account that NSs can spend some significant time (in the case of MFD) at the propeller stage (the spin-down rate at this stage is very uncertain, see the list of formulae, for example, in (Lipunov and Popov, 1995) or (Lipunov, 1992)).

Note that there is another reason for which a very fast decay down to small values of μ_b can also be excluded, as far as this would lead to a huge amount of accreting isolated NSs in drastic contrast with observations. This situation is similar to the "turn-off" of the magnetic field of a NS (i.e., quenching any magnetospheric effect on the accreting matter). So for any velocity and density distributions we should expect significantly more accreting isolated NS than we know from ROSAT observations (of course, for high velocities X-ray sources will be very dim, but close NSs can be observed even for velocities ~ 100 km s^{-1}).

For power-law MFD (contrary to exponential decay) we cannot put serious limits on the parameters of decay with the ROSAT observations of INS candidates as far as for all plausible models of power-law MFD INSs from low velocity tail are able to become accretors. For more detailed conclusions a NS census for power-law MFD is necessary, similar to non-decaying and exponential cases (Popov et al., 2000).

An interesting possibility of observing evolved accreting magnetars appear both for the case of MFD and for constant field evolution. These sources should be different from typical present day INS candidates observed by ROSAT. Existence or absence of old accreting magnetars is very important for the whole NS astrophysics.

We conclude that the existence of several old isolated accreting NSs observed by ROSAT (if it is the correct interpretation of observations), can put important bounds on the models of the MFD for isolated NSs for exponential decay (without influence of accretion, which can stimulate field decay). These models should explain the fact of observations of ~ 10 accreting isolated NSs in the solar vicinity. Here we can not fully discuss the relations between decay parameters and X-ray observations of isolated NSs without detailed calculations. What we showed is that this connection should be taken into account and made some illustrations of it, and future investigations in that field would be desirable.

Acknowledgements We thank Monica Colpi, Denis Konenkov, Konstantin Postnov, George Pavlov and Roberto Turolla for comments on the text and discussions. We want to thank Vladimir Lipunov and Aldo Treves for advices and attention to our work.

We also thank University of Milan, University of Padova, University of Como and Brera Observatory (Merate) for hospitality.

This work was supported by the RFBR (98-02-16801) and the INTAS (96-0315) grants.

References

[1] Alpar, M.A., "Isolated thermal neutron stars, SGRs and AXPs: propellers and early accretors with conventional magnetic fields?", astro-ph/9912228 (1999).

[2] Colpi, M., Geppert, U. and Page, D., "Period clustering of the Anomalous X-ray Pulsars and magnetic field decay in magnetars", *ApJL* **529**, L29 (2000).

[3] Duncan, R.C. and Thompson, C., "Formation of very strongly magnetized neutron stars - Implications for gamma-ray bursts", *ApJ* **392**, L9 (1992).

[4] Geppert, U., Page, D., Colpi, M. and Zannias, T., "Magneto-rotational and thermal evolution of magnetars with crustal magnetic fields", astro-ph/9910563 (1999).

[5] Goldreich, P. and Reisenegger, A., "Magnetic field decay in isolated neutron stars", *ApJ* **395**, 250 (1992).

[6] Gunn, J. and Ostriker, J., "On the Nature of Pulsars. III. Analysis of Observations", *ApJ* **160**, 979 (1970).

[7] Haberl, F., Motch, C. and Pietsch, W., "Isolated neutron stars in the ROSAT Survey", *Astron. Nachr.* **319**, 97 (1998).

[8] Haberl, F., Pietsch, W. and Motch, C., " RX J0420.0-5022: An isolated neutron star candidate with evidence

for 22.7 s X-ray pulsations",
A&A **351**, L53 (2000).

[9] Konar, S. and Bhattacharya, D.,
"Magnetic Fields of Neutron Stars",
astro-ph/9911239 (1999).

[10] Konenkov, D.Yu. and Popov, S.B.,
"RX J0720.4-3125 as a possible example of magnetic field decay in neutron stars",
Astronomy Letters **23**, 200 (1997).

[11] Kouveliotou, C. et al.,
"Discovery of a magnetar associated with the Soft Gamma Repeater SGR 1900+14",
ApJ **510**, L115 (1999).

[12] Lipunov, V.M.,
"Astrophysics of Neutron Stars",
New York: Springer– Verlag (1992).

[13] Lipunov, V.M. and Popov, S.B.,
"Spin Evolution of Isolated Neutron Stars - Spindown Theorem",
AZh **71**, 711 (1995).

[14] Lorimer, D.R., Bailes, M. and Harrison, P. A.,
"Pulsar statistics - IV. Pulsar velocities",
MNRAS **289**, 592 (1997).

[15] Lyne, A.G. and Lorimer, D.R.,
"High Birth Velocities of Radio Pulsars",
Nature **369**, 127 (1994).

[16] Lyne, A.G. et al.,
"The Parkes Southern Pulsar Survey - II. Final results and population analysis",
MNRAS, **295**, 743 (1998).

[17] Marsden, D., Lingenfelter, R.E., Rothschild, R.E. and Higdon, J.C.,
"Nature vs. Nurture: The Origin of Soft Gamma-ray Repeaters and

Anomalous X-ray Pulsars”,
astro-ph/9912207 (1999).

[18] Mereghetti, S. and Stella, L.,
”The very low mass X-ray binary pulsars: A new class of sources?”,
ApJ **442**, L17 (1995).

[19] Mereghetti, S.,
”The Anomalous X-ray Pulsars”,
astro-ph/9911252 (1999).

[20] Neühauser, R. and Trümper, J.E.,
”On the number of accreting and cooling isolated neutron stars detectable with the ROSAT All-Sky Survey”,
A&A, **343**, 151 (1999).

[21] Perna, R., Hernquist, L. and Narayan, R.,
”Emission Spectra of Fallback Disks Around Young Neutron Stars”,
astro-ph/9912297 (1999).

[22] Popov, S.B. and Prokhorov, M.E.,
”ROSAT X-ray sources and exponential field decay in isolated neutron stars”,
A&A in press (2000a).

[23] Popov, S.B. and Prokhorov, M.E.,
”Restrictions on parameters of power-law magnetic field decay for accreting isolated neutron stars”
astro-ph/0001005 (2000b).

[24] Popov, S.B. and Konenkov, D.Yu.,
”Magnetic field decay and period evolution of the source RX J0720.4-3125”,
Radiofizika **41**, 28 (1998).

[25] Popov, S.B. et al.,
”The Neutron Star Census”,
ApJ **530**, 896 (2000).

[26] Sang, Y. and Chanmugam, G.,
"Pulsar statistics with nonexponential magnetic field decay",
ApJ **363**, 597 (1990).

[27] Schwope, A.D., Hasinger, G., Schwarz, R., Haberl, F. and Schmidt, M.,
"The isolated neutron star candidate RBS1223 (1RXS J130848.6+212708)",
A&A, **341**, L51 (1999).

[28] Urpin, V. and Muslimov, A.,
"Crustal magnetic field decay and neutron star cooling",
MNRAS **256**, 261 (1992).

[29] Treves, A., Turolla, R., Zane, S. and Colpi, M.,
"Isolated Neutron Stars: Accretors and Coolers",
PASP **112**, 297 (2000).

[30] Urpin, V.A., Geppert, U. and Konenkov, D.Yu.,
"Wind accretion and magnetorotational evolution of neutron stars in binaries",
A&A **307**, 807 (1996).

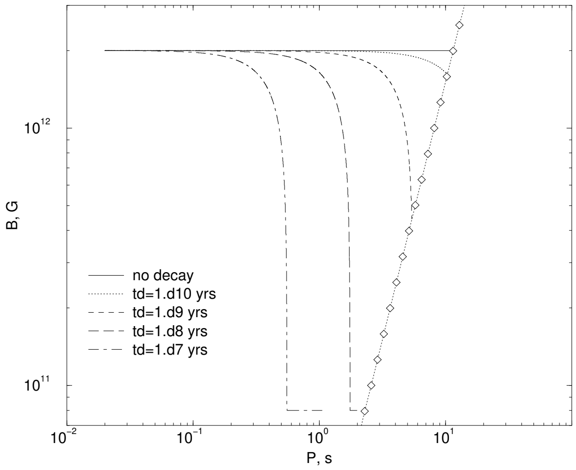

Figure 1: Tracks on P-B diagram. Tracks are plotted for bottom polar magnetic field $8 \cdot 10^{10}$ G, initial polar field $2 \cdot 10^{12}$ G, NS velocity $10\,\mathrm{km s^{-1}}$, ISM density $1\,\mathrm{cm^{-3}}$ and different t_d. The last point of tracks with different t_d corresponds to the following NS ages: 10^{10} yrs for $t_d = 10^7$ and $t_d = 10^8$ yrs; 1.5×10^9 yrs for $t_d = 10^9$ yrs; $\sim 2 \cdot 10^9$ yrs for $t_d = 10^{10}$ yrs. The initial period is assumed to be $p_0 = 0.020$ s. The line with diamonds shows the ejector period, p_E.

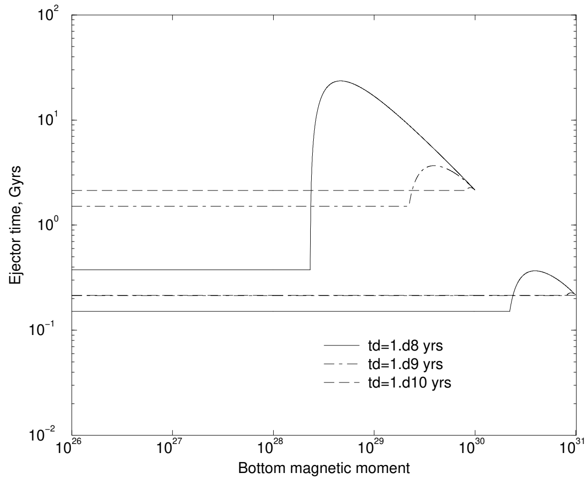

Figure 2: Ejector time t_E (in billion years) vs. the bottom value of the magnetic moment. The curves are shown for two values of the initial magnetic moment: $10^{30}\,\mathrm{G\,cm^3}$ (upper curves) and $10^{31}\,\mathrm{G\,cm^3}$.

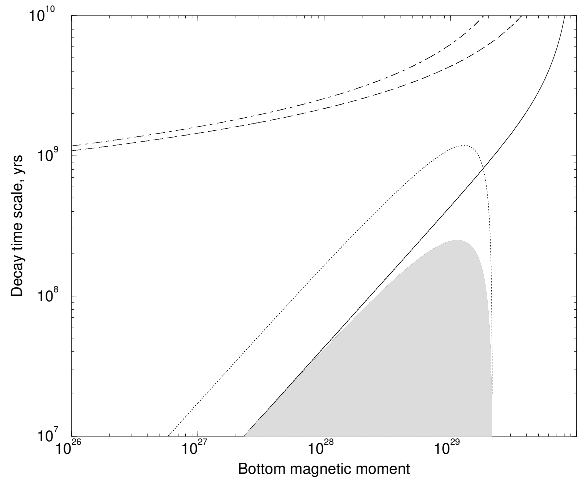

Figure 3: The characteristic time scale of the MFD, t_d, vs. bottom magnetic moment, μ_b. In the hatched region t_E is greater than 10^{10}yrs. The dashed line corresponds to $t_H = t_d \cdot \ln(\mu_0/\mu_b)$, where $t_H = 10^{10}$ years. The solid line corresponds to $p_E(\mu_b) = p(t = t_{cr})$, where $t_{cr} = t_d \cdot \ln(\mu_0/\mu_b)$. Both the lines and hatched region are plotted for $\mu_0 = 10^{30}\,\mathrm{G\,cm^{-3}}$. The dash-dotted line is the same as the dashed one, but for $\mu_0 = 5 \cdot 10^{29}\,\mathrm{G\,cm^3}$. The dotted line shows the border of the "forbidden" region for $\mu_0 = 5 \cdot 10^{29}\,\mathrm{G\,cm^3}$.

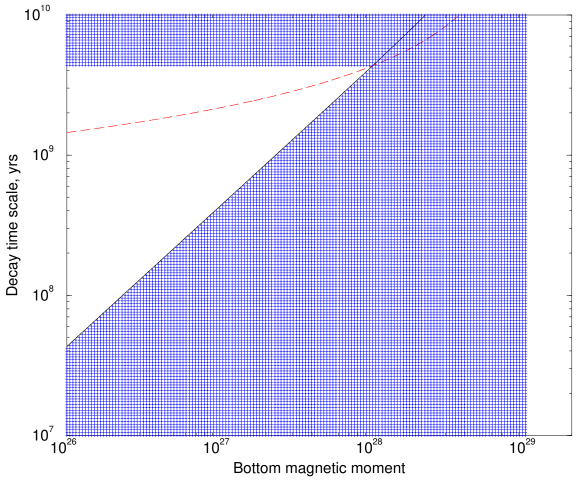

Figure 4: The characteristic time scale of the MFD, t_d, vs. bottom magnetic moment, μ_b. In the hatched region t_E is greater than 10^{10} yrs. The dashed line corresponds to $t_H = t_d \cdot \ln(\mu_0/\mu_b)$, where $t_H = 10^{10}$ yrs. The solid line corresponds to $p_E(\mu_b) = p(t = t_{cr})$, where $t_{cr} = t_d \cdot \ln(\mu_0/\mu_b)$. Both lines and region are plotted for $\mu_0 = 10^{29}\,\mathrm{G\,cm^{-3}}$.

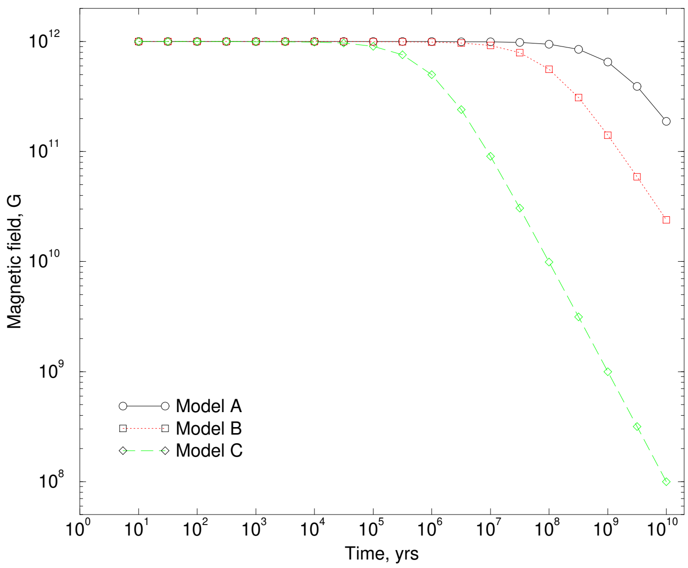

Figure 5: Power-law MFD. Model A: $a = 0.01, \alpha = 1.25$; solid line with circles. Model B: $a = 0.15, \alpha = 1.25$; dashed line with squares. Model C: $a = 10$, $\alpha = 1$; long-dashed line with diamonds. Models were described in details in Colpi et al. (2000) (see also Table 1).

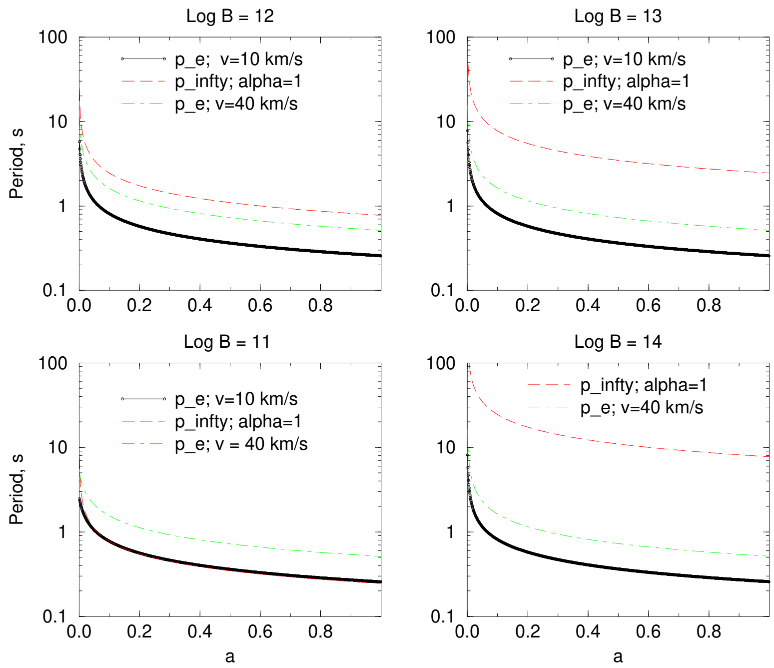

Figure 6: Periods vs. parameter a for different values of the initial magnetic field: $10^{11}, 10^{12}, 10^{13}, 10^{14}$ G.